Hindawi Publishing Corporation
Discrete Dynamics in Nature and Society
Volume 2013, Article ID 239039, 7 pages
http://dx.doi.org/10.1155/2013/239039

Research Article

A Hybrid Temporal-Spatio Forecasting Approach for Passenger Flow Status in Chinese High-Speed Railway Transport Hub

Zhengyu Xie,[1,2] Limin Jia,[2] Yong Qin,[2] and Li Wang[1]

[1] *School of Traffic and Transportation, Beijing Jiaotong University, Beijing 100044, China*
[2] *State Key Laboratory of Rail Traffic Control and Safety, Beijing Jiaotong University, Beijing 100044, China*

Correspondence should be addressed to Limin Jia; jialm@vip.sina.com

Received 16 July 2013; Revised 4 October 2013; Accepted 18 October 2013

Academic Editor: Wuhong Wang

With the rapid development of high-speed railway in China, high-speed railway transport hub (HRTH) has become the high-density distribution center of passenger flow. In order to accurately detect potential safety hazard hidden in passenger flow, it is necessary to forecast the status of passenger flow. In this paper, we proposed a hybrid temporal-spatio forecasting approach to obtain the passenger flow status in HRTH. The approach combined temporal forecasting based on radial basis function neural network (RBF NN) and spatio forecasting based on spatial correlation degree. Computational experiments on actual passenger flow status from a specific bottleneck position and its correlation points in HRTH showed that the proposed approach is effective to forecast the passenger flow status with high precision.

1. Introduction

As main influence factors for the safety and sustainability of transportation system, the insecure behaviors and statuses of people are hot issues and difficult problems in traffic safety engineering [1, 2]. With the rapid development of high-speed railway in China, HRTH has become an interface of multitransportation which includes high-speed railway, civil aviation, highway, waterway, urban rail transit, public transport, and private vehicles, and the safety of passenger flow in HRTH has attracted more and more attention. As the vital node of passenger transport net, HRTH is an important collection and distribution center of various transportation modes and massive passenger flow. The distribution quantity of passengers will be sustained to sharply increase with the growth of high-speed railway operation mileage. As the dramatic increase of passengers, high-density passenger flow is generated, which imposed a rigorous challenge to the safety management of HRTH.

In order to avoid and solve the problems caused by passenger flow abnormal status, many approaches are proposed in literatures which can be mainly classified into two categories. The first category is the studies on passenger flow modeling and simulating in transport hubs. Gipps and Marksjö [3] focused on the prediction the alteration passenger flow in the passing environment and proposed a model for the interactions between passengers which is intended for use in a graphical computer simulation. Seyfried et al. [4] analyzed the influence of various approaches for the interaction between the passengers on the resulting velocity-density relation based on a modified social force model. Jia et al. [5] analyzed the characteristics of passenger flow and present parameters relation models for passenger flow on different terminal facilities were established based on data statistics. Ji et al. [6] proposed a cell-based model including two steps. The first step is to update speed, which is the cells the passenger can move in one time interval and the other is to analyze the overtaking. Wang et al. [7] simulated the passenger flow in a station hall during the spring festival by modifying the social force model. According to the studies on the first category, decision makers can adjust layout and distribution of facilities and equipment in transport hub to adapt to the modeling and simulating results of passenger

flow. This category studies aim at decreasing and preventing passenger flow abnormal status before they happened.

The other category focuses on the modeling and simulating of congestion evacuations which are caused by high-density passenger flow. Zhong et al. [8] introduced the passenger evacuation design in the construction of metros in China and proposed a dynamic model to simulate the passenger evacuation. Jiang et al. [9] studied the effect of varying maximum upstairs speed and the average minimum width of staircase utilized per person by taking two subway stations in China as examples. VanLandegen and Chen [10] integrated a pedestrian model with a Metrorail transit model to evaluate the performance of the Metrorail in the hypothetical large-scale evacuations. Shi et al. [11] firstly investigated and established the safety strategy of evacuation in metro stations, which involves the occupants needed to be evacuated, the evacuation route, and the safety zone. Based on the studies on the second category, decision makers can make an efficient emergency evacuation decision to determine routes and channels of evacuation. This category studies aim at mitigating passenger flow abnormal status after they happened.

According to the literature review above, most studies focus on solving approaches before or after passenger flow abnormal status happened. Specific literature on real-time changing process of passenger flow status is scarce because of limitation from the difficult acquisition of real-time passenger flow status. With the widespread applications of intelligent video surveillance in Chinese HRTH, real-time acquisition of passenger flow status has become feasible. In this paper, passenger flow status is defined as the amount, velocity, and density of passenger flow. We consider the real-time passenger flow status in bottleneck positions of HRTH and propose a hybrid temporal-spatio forecasting approach to reflect the change of passenger flow status.

The rest of paper is organized as follows: a hybrid temporal-spatio forecasting approach for passenger flow status of bottleneck positions is developed in Section 2. Computational results are reported in Section 3 and finally Section 4 covers the conclusion.

2. A Hybrid Temporal-Spatio Forecasting Approach

A hybrid forecasting approach for passenger flow status of bottleneck positions is proposed in this section, which combines temporal and spatio forecasting methods. A temporal forecasting based on RBF NN is proposed to forecast passenger flow status of bottleneck position by using the real-time passenger flow status of the position. The temporal forecasting method can rapidly and precisely reflect the passenger flow status in the bottleneck position but is insensitive for the passenger flow fluctuation from correlation points. So we introduce a spatio forecasting approach based on spatial correlation degree to combine with the temporal forecasting approach for improving the forecasting precision.

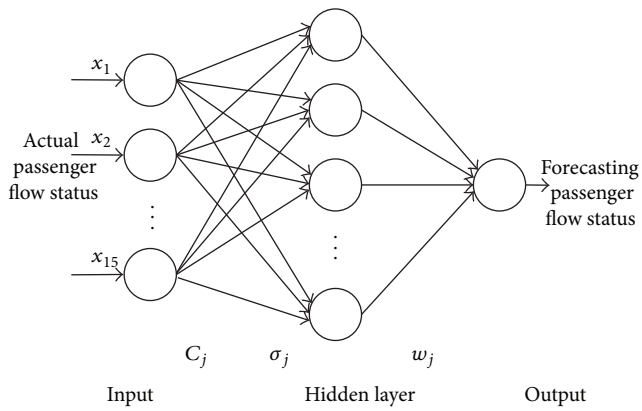

Figure 1: Structure of RBF NN.

2.1. Temporal Forecasting Based on RBF NN. The RBF NN is a typical feed-forward neural network, which has many merits, such as nonlinear mapping characteristics, self-organized study ability, training fast, and the capability of converging in global optimization and approaching the function in the best way. Simply for its great advantages, RBF NN has been applied in many fields [12–15]. A temporal forecasting approach based on RBF NN is proposed in this section to forecast passenger flow status of bottleneck positions in HRTH.

2.1.1. Design of RBF NN. The structure of RBF NN is comprised of three different layers: an input layer, a hidden layer and an output layer. The structure of RBF NN for temporal forecasting is shown in Figure 1.

The input vector $X = (x_1, x_2, \ldots, x_{15})$ is composed of the input signals x_i, and there are fifteen input neurons in our RBF NN. The output $h_j(X)$ of the jth neuron in the hidden neuron in the hidden layer is described by

$$h_j(X) = \varphi\left(\left\|X - C_j\right\|\right), \tag{1}$$

where $\varphi(\cdot)$ is the radial basis function, $C_j (C_j \in R^n)$ is the center of the jth hidden neuron, and $\|\cdot\|$ is the Euclidean norm. In our RBF NN, $\varphi(\cdot)$ is adopted to be the Gaussian function, and $h_j(X)$ is described by

$$h_j(X) = \exp\left(-\frac{\left\|X - C_j\right\|^2}{2\sigma_j^2}\right), \tag{2}$$

where σ_j is the spread of the jth hidden neuron for the ith input signal.

The output $Y(X)$, which is designed as passenger flow status forecasting, is the linearly combined signal of the outputs $h_j(X)$ from the hidden layer with the synaptic weights $w_j$described by

$$Y(X) = \sum_{j=1}^{m} w_j h_j(X), \tag{3}$$

where m is the number of hidden neurons.

Table 1: Mapping structure between input variables and output variable.

Input variables	Output variable
$x_1, x_2, \ldots, x_{15}$	x_{16}
$x_2, x_3, \ldots, x_{16}$	x_{17}
$\vdots$	$\vdots$
$x_{l-15}, x_{l-14}, \ldots, x_{l-1}$	x_l

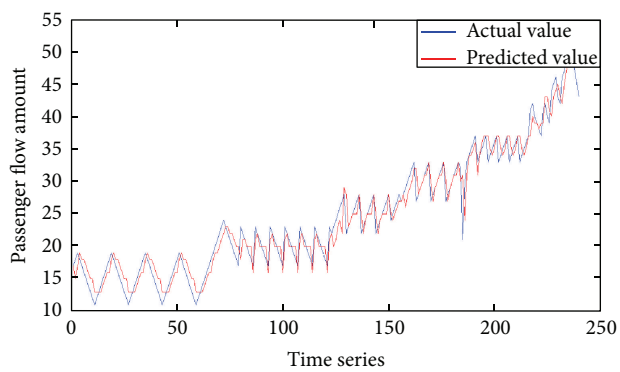

Figure 2: Comparison between actual value and forecasting value based on RBF NN.

Table 2: Input and output values.

No.	Input value	Output value
1	−0.7561 −0.8537 0.9024 0.8537 −1.0000 −0.9512 −0.9024 −0.8537 −0.8049 −0.7561 −0.7073 −0.6585 −0.6098 −0.6585 −0.7073	−0.7561
2	−0.8537 0.9024 0.8537 −1.0000 −0.9512 −0.9024 −0.8537 −0.8049 −0.7561 −0.7073 −0.6585 −0.6098 −0.6585 −0.7073 −0.7561	−0.8049
3	0.9024 0.8537 −1.0000 −0.9512 −0.9024 −0.8537 −0.8049 −0.7561 −0.7073 −0.6585 −0.6098 −0.6585 −0.7073 −0.7561 −0.8049	−0.8537
$\vdots$	$\vdots$	$\vdots$
234	0.5122 0.4146 0.3659 0.6098 0.6585 0.7073 0.5610 0.5122 0.7073 0.7561 0.9512 0.9024 1.0000 0.8537 0.7561	0.6585
235	0.4146 0.3659 0.6098 0.6585 0.7073 0.5610 0.5122 0.7073 0.7561 0.9512 0.9024 1.0000 0.8537 0.7561 0.6585	0.5610

2.1.2. Input Variables Determined. It is very important to select proper input variables for a neural network. On the one hand, as the number of the input variables increases, the NN architecture will be larger and the computing time will be longer. On the other hand, the irrelevant or mutually correlated input variables are not useful for improving the prediction accuracy. Therefore, how to select a few but sufficient input variables is a key issue.

According to plenty of experiments on the input variables, we choose passenger flow status (amount, velocity, or density) of 15 points in the time series as the variables input our RBF NN and passenger flow status (amount, velocity, or density) of the point after the 15th point as the output variable. $X = \{x_i \mid x_i \in N^+, i = 1, 2, \ldots, l\}$ is a time series set and x_i is the passenger flow status (amount, velocity, or density) of the ith point in the time series. The mapping structure between input variables and output variable is shown in Table 1.

2.1.3. RBF NN Testing. In order to test the accuracy of temporal forecasting, we choose 250 actual passenger flow amounts of one bottleneck position in time series as testing samples. The input and output values after normalization are shown in Table 2.

A comparison between actual value and forecasting value based on RBF NN is shown in Figure 2. The average precision of forecasting is 94.14%. The testing result indicates that the RBF NN has a desirable performance on forecasting.

2.2. Spatio Forecasting Based on Spatial Correlation Degree. According to the spatial correlation degree and passenger flow status of bottleneck position P_0 and its correlation points C_i, a spatio forecasting model is proposed to forecast the passenger flow status of bottleneck position P_0.

2.2.1. Analysis of Spatial Correlation Degree. $X_i = \{x_i(k) \mid k = 1, 2, \ldots, n\}$ $(i = 1, 2, \ldots, m)$ is a sequence set, $x_0(k)$ is a reference sequence, and $x_i(k)$ is comparison sequence. $r(x_0(k), x_i(k))$ is the correlation coefficient of comparison sequence relative to reference sequence at period k, as shown in (4). Consider

$$r\left(x_0(k), x_i(k)\right) = \frac{\min_i \min_k \left|x_0(k) - x_i(k)\right| + \zeta \max_i \max_k \left|x_0(k) - x_i(k)\right|}{\left|x_0(k) - x_i(k)\right| + \zeta \max_i \max_k \left|x_0(k) - x_i(k)\right|}, \quad (4)$$

where ζ is the discriminating coefficient, $\zeta \in (0, 1)$.

$r(x_0, x_i)$ is the correlation degree of the ith comparison sequence x_i relative to reference sequence x_0, as shown in (5). Consider

$$r\left(x_0, x_i\right) = \frac{1}{n} \sum_{k=1}^{n} r\left(x_0(k), x_i(k)\right). \quad (5)$$

α_i is the correlation weight coefficient and is described by (6). Consider

$$\alpha_i = \frac{r\left(x_0, x_i\right)}{\sum_{j=1}^{n} r\left(x_0, x_j\right)}. \quad (6)$$

2.2.2. Spatio Forecasting Model. According to the passenger flow status of C_i and the spatio correlation degree between P_0

and C_i, the passenger flow status of P_0 is forecasted based on spatio forecasting model. The initial forecasting value $x_c{}'(t)$ of P_0 at period t is calculated by (7). Consider

$$x_c{}'(t) = \sum_{i=1}^{n} \alpha_i x_i (t - t_i), \tag{7}$$

where $x_i(t)$ is passenger flow status of C_i at period t, t_i is the average moving time from C_i to P_0, and α_i is the correlation weight coefficient between correlated points C_i and congested point P_0. According to (6), α_i is described by

$$\alpha_i = \frac{r(P_0, C_i)}{\sum_{j=1}^{n} r(P_0, C_i)}, \tag{8}$$

where $r(P_0, C_i)$ is the correlation degree of between C_i and P_0.

In order to reduce the errors which are caused by uncertainties passenger flow status, we use the change of initial forecasting value $x_c{}'(t)$ and actual passenger flow status value $x_c(0)$ of P_0 at the beginning of period t to describe the forecasting value $x_c(t)$ of P_0 at period t. The spatio forecasting model of passenger flow status is shown in (9). Consider

$$x_c(t) = \sum_{i=1}^{n} \alpha_i x_i (t - t_i) - \sum_{i=1}^{n} \alpha_i x_i (0) + x_c(0). \tag{9}$$

The velocity in correlated points prominently affects the density of congested point; the faster the velocity of correlated points, the weaker affection on the density of congested point. So we adopt velocity to improve the density forecasting. The spatio forecasting model of passenger flow density is shown in (10). Consider

$$x_{\rho c}(t) = \sum_{i=1}^{n} \frac{k v_i (t - t_i)}{v_0 (t - t_i)} \alpha_i x_{\rho i} (t - t_i) - \sum_{i=1}^{n} \alpha_i x_{\rho i}(0) + x_\rho(0), \tag{10}$$

where $x_{\rho c}(t)$ is the forecasting passenger flow density of P_0 at period t, $v_i(t - t_i)$ is the velocity of correlated points at period $t - t_i$, $v_0(t - t_i)$ is the velocity of congested point at period $t - t_i$, and $x_\rho(0)$ is the actual density of P_0 at the beginning of period t.

Similarly, the density in correlated points prominently affects the velocity of congested point; the higher the density of correlated points, the faster the velocity of congested point. So, we adopt density to improve the velocity forecasting. The spatio forecasting model of passenger flow velocity is shown in (11). Consider

$$x_{vc}(t) = \sum_{i=1}^{n} \frac{k \rho_0 (t - t_i)}{\rho_i (t - t_i)} \alpha_i x_{vi} (t - t_i) - \sum_{i=1}^{n} \alpha_i x_{vi}(0) + x_v(0), \tag{11}$$

where $x_{vc}(t)$ is the forecasting passenger flow velocity of P_0 at period t, $\rho_i(t - t_i)$ is the density of correlated points at period $t - t_i$, $\rho_0(t - t_i)$ is the density of congested point at period $t - t_i$, and $x_v(0)$ is the actual velocity of P_0 at the beginning of period t.

2.3. Temporal-Spatio Forecasting Combination. A hybrid forecasting approach to combine the spatio and temporal forecasting is proposed in this section. The forecasting value $x_r(t)$ based on RBF NN and the forecasting value $x_c(t)$ based on spatioforecasting model are combined by a linear regression model, which is shown in (12). Consider

$$f(t) = \beta_1 x_r(t) + \beta_2 x_c(t) + \beta_3. \tag{12}$$

The parameters of the model are determined by numerical fitting of actual passenger flow status values and forecasting values generated by spatio and temporal forecasting methods.

According to the spatio and temporal forecasting methods and the combination model, the temporal-spatio forecasting model of passenger flow density is described by

$$f_\rho(t) = \beta_{\rho 1} x_{\rho r}(t) + \beta_{\rho 2} \left[\sum_{i=1}^{n} \frac{k v_i (t - t_i)}{v_0 (t - t_i)} \alpha_i x_{\rho i} (t - t_i) - \sum_{i=1}^{n} \alpha_i x_{\rho i}(0) + x_\rho(0) \right] + \beta_{\rho 3}. \tag{13}$$

According to the spatio and temporal forecasting methods and the combination model, the temporal-spatio forecasting model of passenger flow velocity is described by

$$f_v(t) = \beta_{v1} x_{vr}(t) + \beta_{v2} \left[\sum_{i=1}^{n} \frac{k \rho_0 (t - t_i)}{\rho_i (t - t_i)} \alpha_i x_{vi} (t - t_i) - \sum_{i=1}^{n} \alpha_i x_{vi}(0) + x_v(0) \right] + \beta_{v3}. \tag{14}$$

3. Computational Experiments

To illustrate the proposed forecasting approach, computational experiments are performed by using the actual passenger flow status from a specific bottleneck position in the Chinese HRTH. In order to assess the improvement of our approach, the forecasting of passenger flow density and velocity among temporal forecasting based on RBF NN, spatio forecasting based on spatial correlation degree, and hybrid temporal-spatio forecasting approach are compared. These numerical experiments are performed based on a personal computer with Intel Core(TM) i5-2450M @ 2.50 GHz processors and 4 GB RAM.

To implement the proposed forecasting approach, the parameters related to specific bottleneck position of HRTH are needed. The specific bottleneck position is a ticket entrance P with 3 correlation points A, B, and C. The average passenger moving time of A to P is 35 s, B to P is 55 s, and C to P is 20 s. We choose 311 data of passenger flow density and 311 data of passenger flow velocity as the computational examples.

According to RBF NN designed in Section 2, temporal forecasting experiments on passenger flow density and

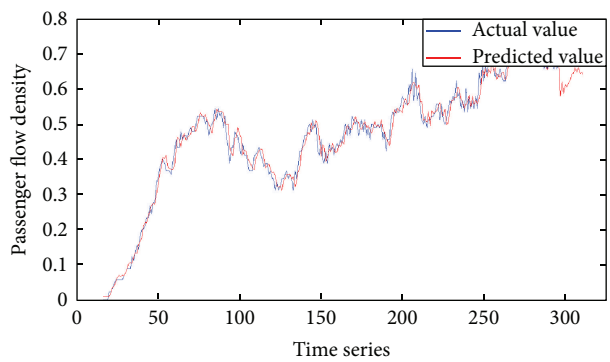

FIGURE 3: Comparison between actual value and forecasting value of passenger flow density based on RBF NN.

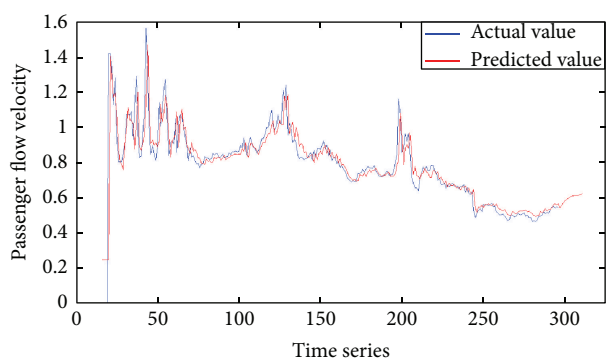

FIGURE 4: Comparion between actual value and forecasting value of passenger flow velocity based on RBF NN.

velocity are implemented. The comparison between actual value and forecasting value of passenger flow density based on RBF NN is shown in Figure 3 and comparison between actual value and forecasting value of passenger flow velocity based on RBF NN is shown in Figure 4.

According to spatio forecasting model proposed in Section 2, spatio forecasting experiments on passenger flow density and velocity are implemented. x_0 is the passenger flow status sequence of P, x_1 is the passenger flow status sequence of A, x_2 is the passenger flow status sequence of B, and x_3 is the passenger flow status sequence of C. The spatial correlation degrees are calculated according to (4) and (5). The calculation result is shown as follows:

$$r(0,1) = 0.510, \quad r(0,2) = 0.761, \quad r(0,3) = 0.404. \tag{15}$$

The forecasting value of passenger flow density based on spatio forecasting model is calculated by (16) and the

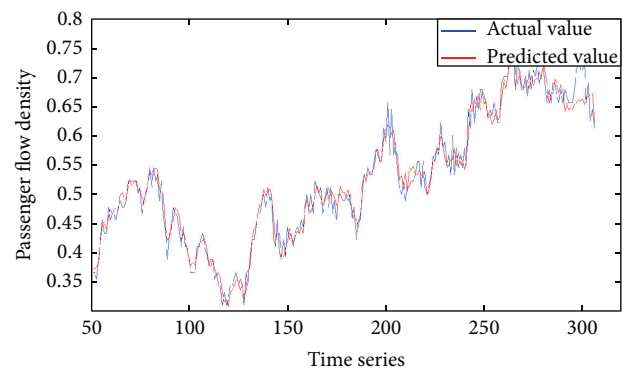

FIGURE 5: Comparion between actual value and forecasting value of passenger flow density based on spatio forecasting model.

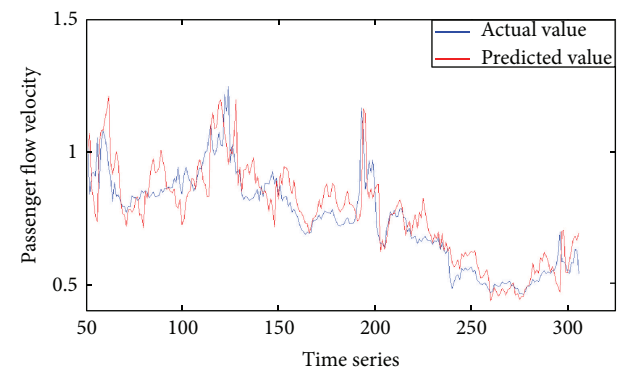

FIGURE 6: Comparion between actual value and forecasting value of passenger flow velocity based on spatio forecasting model.

forecasting value of passenger flow velocity based on spatio forecasting model is calculated by (17). Consider

$$\begin{aligned} x_{\rho c}(t) &= \sum_{i=1}^{n} \frac{k\nu_i}{\nu_0} \alpha_i x_{\rho i}(t - t_i) - \sum_{i=1}^{n} \alpha_i x_{\rho i}(0) + x_\rho(0) \\ &= \frac{0.304\nu_1}{\nu_0} x_{\rho 1}(t-35) + \frac{0.454\nu_2}{\nu_0} x_{\rho 2}(t-55) \\ &\quad + \frac{0.241\nu_3}{\nu_0} x_{\rho 3}(t-20) + 0.206, \end{aligned} \tag{16}$$

$$\begin{aligned} x_{\nu c}(t) &= \sum_{i=1}^{n} \frac{k\rho_0}{\rho_i} \alpha_i x_{\nu i}(t - t_i) - \sum_{i=1}^{n} \alpha_i x_{\nu i}(0) + x_\nu(0) \\ &= \frac{0.213\rho_1}{\rho_0} x_{\nu 1}(t-35) + \frac{0.363\rho_2}{\rho_0} x_{\nu 2}(t-55) \\ &\quad + \frac{0.193\rho_3}{\rho_0} x_{\nu 3}(t-20) + 0.671. \end{aligned} \tag{17}$$

The comparison between actual value and forecasting value of passenger flow density based on spatio forecasting model is shown in Figure 5 and comparison between actual value and forecasting value of passenger flow velocity based on spatioforecasting model is shown in Figure 6.

Table 3: Average forecasting precision comparison of three approaches.

Forecasting approach	Average forecasting precision of density	Average CPU time of density forecasting (s)	Average forecasting precision of velocity	Average CPU time of velocity forecasting (s)
Temporal forecasting approach based on RBF NN	95.21%	9.8	94.73%	9.6
Spatio forecasting approach based on spatial correlation degree	91.23%	11.2	88.21%	12.1
Hybrid temporal-spatio forecasting approach	96.83%	12.9	96.10%	13.7

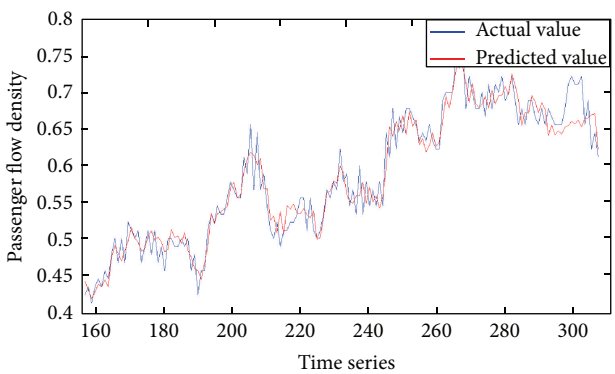

Figure 7: Comparion between actual value and forecasting value of passenger flow density based on hybrid temporal-spatio forecasting approach.

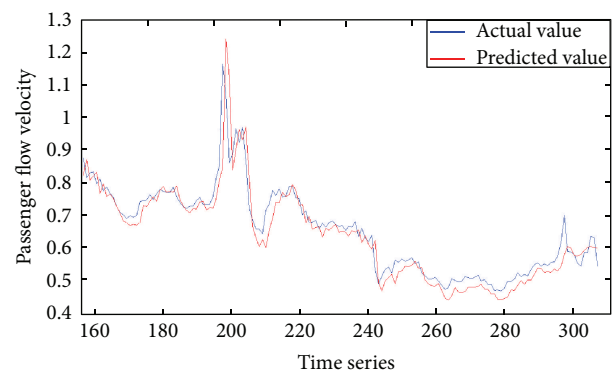

Figure 8: Comparion between actual value and forecasting value of passenger flow velocity based on hybrid temporal-spatio forecasting approach.

Based on the numerical fitting of actual and forecasting passenger flow status value in P, the forecasting value of passenger flow density based on hybrid temporal-spatio forecasting approach is calculated by (18) and the forecasting value of passenger flow velocity based on hybrid temporal-spatio forecasting approach is calculated by (19). Consider

$$\begin{aligned} x_\rho(t) = {} & 0.889 x_{\rho r}(t) + \frac{0.034\nu_1}{\nu_0} x_{\rho 1}(t-25) \\ & + \frac{0.050\nu_2}{\nu_0} x_{\rho 2}(t-55) \\ & + \frac{0.0271\nu_3}{\nu_0} x_{\rho 3}(t-20) + 0.022, \end{aligned} \tag{18}$$

$$\begin{aligned} x_\nu(t) = {} & 0.903 x_{\nu r}(t) + \frac{0.020\rho_1}{\rho_0} x_{\nu 1}(t-35) \\ & + \frac{0.035\rho_2}{\rho_0} x_{\nu 2}(t-55) + \frac{0.019\rho_3}{\rho_0} x_{\nu 3}(t-20) + 0.044. \end{aligned} \tag{19}$$

The comparison between actual value and forecasting value of passenger flow density based on hybrid temporal-spatio forecasting approach is shown in Figure 7 and comparison between actual value and forecasting value of passenger flow velocity based on hybrid temporal-spatio forecasting approach is shown in Figure 8.

The average forecasting precision comparison of three approaches mentioned above is shown in Table 3.

As observed in Table 3, the hybrid temporal-spatio forecasting approach proposed in this paper has the higher forecasting precisions than temporal and spatio forecasting approaches under the similar computation complexity. The results of computational experiments indicate that our approach is effective to forecast the passenger flow status of bottleneck positions in Chinese HRTH.

4. Conclusion

In this paper, we considered the forecasting approach for passenger flow status in the Chinese HRTH. A hybrid temporal-spatio forecasting approach was proposed, which combined temporal forecasting and spatio forecasting. The temporal forecasting based on RBF NN could fast and accurately forecast the status change of passenger flow but was insensitive for the influences from correlation points. A spatio forecasting approach based on spatial correlation degree was introduced to combine with the temporal forecasting approach to avoid the influences and improve the forecasting precision. Computational experiments on the actual passenger flow density and velocity from a specific bottleneck position and its correlation points in Chinese HRTH showed that the approach proposed in this paper is effective to forecast the passenger flow status of bottleneck position in HRTH with high forecasting precision for different types of passenger flow status. In the future, considering the passenger flow abnormal status forewarning of bottleneck position

based on the passenger flow status forecasting is a possibility for further research.

Conflict of Interests

The authors declare that there is no conflict of interests regarding the publication of this paper.

Acknowledgment

This research was supported by a Grant (no. I11A300010) from the National Natural Science Foundation of China.

References

[1] W. Wang, W. Zhang, H. Guo, H. Bubb, and K. Ikeuchi, "A safety-based approaching behavioural model with various driving characteristics," *Transportation Research C*, vol. 19, no. 6, pp. 1202–1214, 2011.

[2] H. Guo, W. Wang, W. Guo, X. Jiang, and H. Bubb, "Reliability analysis of pedestrian safety crossing in urban traffic environment," *Safety Science*, vol. 50, no. 4, pp. 968–973, 2012.

[3] P. G. Gipps and B. Marksjö, "A micro-simulation model for pedestrian flows," *Mathematics and Computers in Simulation*, vol. 27, no. 2-3, pp. 95–105, 1985.

[4] A. Seyfried, B. Steffen, and T. Lippert, "Basics of modelling the pedestrian flow," *Physica A*, vol. 368, no. 1, pp. 232–238, 2006.

[5] H.-F. Jia, L.-L. Yang, and M. Tang, "Pedestrian flow characteristics analysis and model parameter calibration in comprehensive transport terminal," *Journal of Transportation Systems Engineering and Information Technology*, vol. 9, no. 5, pp. 117–123, 2009.

[6] X. Ji, X. Zhou, and B. Ran, "A cell-based study on pedestrian acceleration and overtaking in a transfer station corridor," *Physica A*, vol. 392, no. 8, pp. 1828–1839, 2013.

[7] L. Wang, Q. Zhang, Y. Cai, J. L. Zhang, and Q. G. Ma, "Simulation study of pedestrian flow in a station hall during the spring festival travel rush," *Physica A*, vol. 392, no. 10, pp. 2470–2478, 2013.

[8] M. Zhong, C. Shi, X. Tu, T. Fu, and L. He, "Study of the human evacuation simulation of metro fire safety analysis in China," *Journal of Loss Prevention in the Process Industries*, vol. 21, no. 3, pp. 287–298, 2008.

[9] C. S. Jiang, F. Yuan, and W. K. Chow, "Effect of varying two key parameters in simulating evacuation for subway stations in China," *Safety Science*, vol. 48, no. 4, pp. 445–451, 2010.

[10] L. D. VanLandegen and X. Chen, "Microsimulation of large-scale evacuations utilizing metrorail transit," *Applied Geography*, vol. 32, no. 2, pp. 787–797, 2012.

[11] C. Shi, M. Zhong, X. Nong, L. He, J. Shi, and G. Feng, "Modeling and safety strategy of passenger evacuation in a metro station in China," *Safety Science*, vol. 50, no. 5, pp. 1319–1332, 2012.

[12] J. Bi, S. Shao, W. Guan, and L. Wang, "State of charge estimation of Li-ion batteries in an electric vehicle based on a radial-basis-function neural network," *Chinese Physics B*, vol. 21, no. 11, Article ID 118801, 2012.

[13] W. Y. Chang, "Equivalent circuit parameters estimation for PEM fuel cell using RBF neural network and enhanced particle swarm optimization," *Mathematical Problems in Engineering*, vol. 2013, Article ID 672681, 8 pages, 2013.

[14] E. E. Abusham and E. K. Wong, "Locally linear discriminate embedding for face recognition," *Discrete Dynamics in Nature and Society*, vol. 2009, Article ID 916382, 8 pages, 2009.

[15] J.-D. Wu and J.-C. Liu, "A forecasting system for car fuel consumption using a radial basis function neural network," *Expert Systems with Applications*, vol. 39, no. 2, pp. 1883–1888, 2012.